

SUPPORTING INFORMATION.

Solvated Structure of Cellulose

in a Phosphonate-based Ionic Liquid.

Kazu Hirosawa,¹ Kenta Fujii,^{2} Kei Hashimoto³, and Mitsuhiro Shibayama^{1*}*

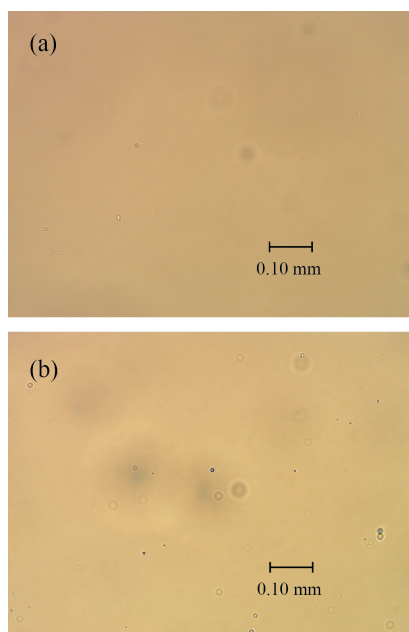
¹ Institute for Solid State Physics, The University of Tokyo, 5-1-5 Kashiwanoha, Kashiwa, Chiba 277-8581, Japan. ² Graduate School of Sciences and Technology for Innovation, Yamaguchi University, 2-16-1 Tokiwadai, Ube, Yamaguchi 755-8611, Japan. ³ Department of Chemistry and Biotechnology, Yokohama National University, 79-5 Tokiwadai, Hodogaya-ku, Yokohama 240-8501, Japan.

AUTHOR EMAIL ADDRESS: k-fujii@yamaguchi-u.ac.jp (K. F.), sibayama@issp.u-tokyo.ac.jp (M. S.)

Section S1: Microscope Observation of Cellulose in $[\text{C}_2\text{mIm}][\text{CH}_3\text{HPO}_3]$ Solutions.

Droplets of the prepared cellulose in $[\text{C}_2\text{mIm}][\text{CH}_3\text{HPO}_3]$ solutions are observed by an optical microscope (BX51N-33P-O-SP, Olympus Co.). Figure S1 shows optical microscope images of neat $[\text{C}_2\text{mIm}][\text{CH}_3\text{HPO}_3]$ and cellulose in $[\text{C}_2\text{mIm}][\text{CH}_3\text{HPO}_3]$ solution of $\phi = 0.047$, which is the highest concentration examined. The cellulose solution looked almost the same as that of neat $[\text{C}_2\text{mIm}][\text{CH}_3\text{HPO}_3]$. It indicated that undissolved cellulose powder granules did not exist in all the cellulose solutions examined in the present study.

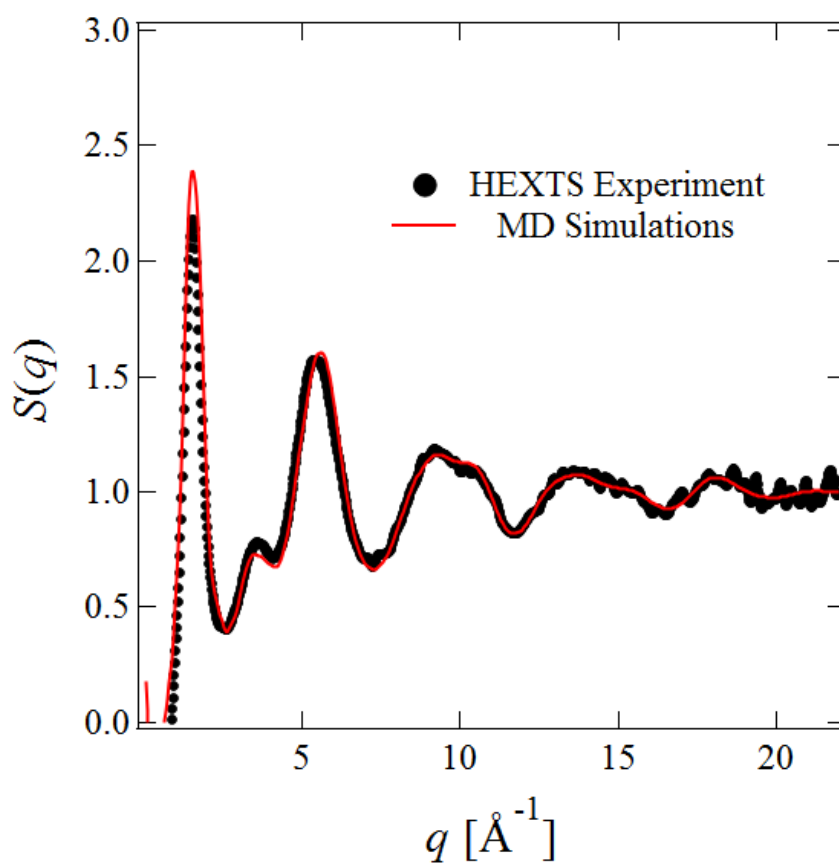
Figure S1.



Optical microscope images of (a) neat $[\text{C}_2\text{mIm}][\text{CH}_3\text{HPO}_3]$ and (b) cellulose in $[\text{C}_2\text{mIm}][\text{CH}_3\text{HPO}_3]$ solution of $\phi = 0.047$. A scale bar of 0.10 mm is also shown in the images.

Section S2: X-ray Structure Factor, $S(q)$ at Whole q -Range.

Figure S2.



X-ray structure factors, $S(q)$ obtained from HEXTS experiments (filled circles) and MD simulations (red solid line) for 30 wt% cellobiose in $[\text{C}_2\text{mIm}][\text{CH}_3\text{HPO}_3]$ solution, at the whole q -range examined.

Section S3: Estimation of the Abundance Ratio of the Intramolecular Hydrogen Bonds within Cellobiose to the Intermolecular Ones between Cellobiose and $\text{CH}_3\text{HPO}_3^-$.

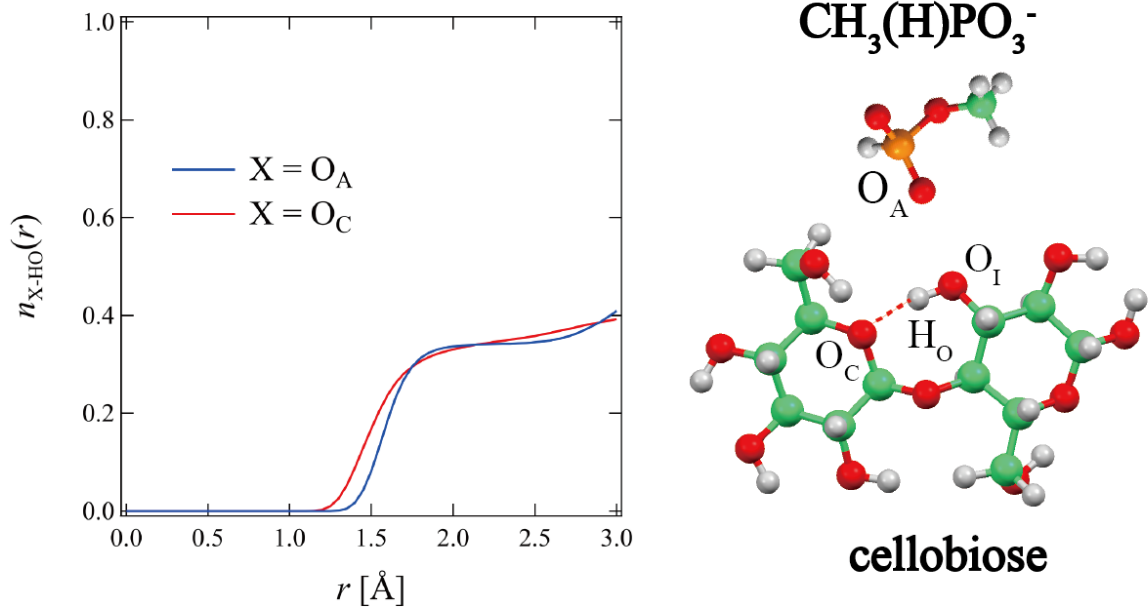
The atom-atom pair correlation function between i -atoms and j -atoms, $g_{i-j}^{\text{MD}}(r)$ is calculated from the MD simulation trajectory according to the following equations:

$$g_{i-j}^{\text{MD}}(r) = \frac{1}{4\pi r^2 \Delta r} \frac{V}{N_i N_j} \left\langle \sum_{m=1}^{n_i} \Delta N_m^{ij}(r) \right\rangle \quad (\text{Intermolecular correlations}) \quad (\text{S1})$$

$$g_{i-j}^{\text{MD}}(r) = \frac{1}{4\pi r^2 \Delta r} \frac{V}{N_i} \left\langle \sum_{m=1}^{n_i} \Delta N_m^{ij}(r) \right\rangle \quad (\text{Intramolecular correlations}) \quad (\text{S2})$$

Here, N_i (N_j) and V denote the total number of i -atoms (j -atoms) and the volume of the MD cell, respectively. $\Delta N_m^{ij}(r)$ is the number of j -atoms in the spherical shell of radius r and thickness Δr centered on a m th i -atom.

Figure S3.



The coordination number of the atoms around Ho, $n_{X-HO}(r)$ ($X = O_A, O_C$).

As mentioned in the main text, the intramolecular hydrogen bonds $O_C \cdots H_O-O_I$ exist in cellobiose molecules dissolved in $[C_2mIm][CH_3HPO_3^-]$. Here, we estimated the abundance ratio of the intramolecular hydrogen bonds, $O_C \cdots H_O-O_I$ to the intermolecular hydrogen bonds, $O_A \cdots H_O-O_I$ from the viewpoint of the coordination number. The coordination number of i -atoms around j -atom is calculated by the following equation;

$$n_{i-j}(r) = \int_0^r \left[\frac{N_i}{V} g_{i-j}^{MD}(r') \right] 4\pi r'^2 dr' \quad (S3)$$

The abundance ratio can be estimated from the ratio of $n_{O_A-HO}(r)$ to $n_{O_C-HO}(r)$ at the first coordination shell. As shown in Figure S3, both of $n_{O_A-HO}(r)$ and $n_{O_C-HO}(r)$ reached a plateau at $r = 2.0$ Å; thus we decided that the outer limit of the first coordination shell is $r = 2.0$ Å. The value of $n_{O_A-HO}(r)$

and $n_{\text{OC-HO}}(r)$ at $r = 2.0 \text{ \AA}$ was 0.34 and 0.33, respectively. Hence, the abundance ratio was found to be $0.33:0.34 = 0.97:1.00$.

Section S4: Calculation of the Collective Diffusion Coefficient: A Partial-heterodyne Method.

A “partial-heterodyne” method in dynamic light scattering analysis has been established for scattering medias which contain frozen heterogeneity, such as polymer gels.¹ The analytical procedures are summarized below. According to the main manuscript, the time correlation function of light scattering intensity at a given measurement point, $g_p^{(2)}(\tau) - 1$ can be approximated as follows:

$$g_p^{(2)}(\tau) - 1 = \beta \sigma_I^2 \left[A \exp(-D_{A,\text{fast},p} q^2 \tau) + (1 - A) \exp(-D_{A,\text{slow},p} q^2 \tau) \right]^2 \quad (\text{S4})$$

where β is the coherence factor. σ_I^2 is related to the fraction of time-averaged scattering intensity originating from thermal fluctuation, $\langle I_F \rangle$ in the total scattering intensity, $\langle I \rangle_p$ as follows:

$$\sigma_I^2 = X_p(2 - X_p) \quad (\text{S5})$$

$$X_p = \frac{\langle I_F \rangle}{\langle I \rangle_p} \quad (\text{S6})$$

When light scattering intensity of sample is comparable with scattering intensity from solvent (I_{back}), we need to subtract I_{back} from $\langle I \rangle_p$ and $\langle I_F \rangle$ in eq. (S6). Then eq. (S6) should be revised as follows:

$$X_p = \frac{\langle I_F \rangle - I_{\text{back}}}{\langle I \rangle_p - I_{\text{back}}} \quad (\text{S7})$$

The apparent diffusion coefficient $D_{A,fast,p}$ is affected by the value of X_p and thus $D_{A,fast,p}$ depends on position. The true collective diffusion coefficient D_{fast} can be estimated from $D_{A,fast,p}$ using the following relationship.

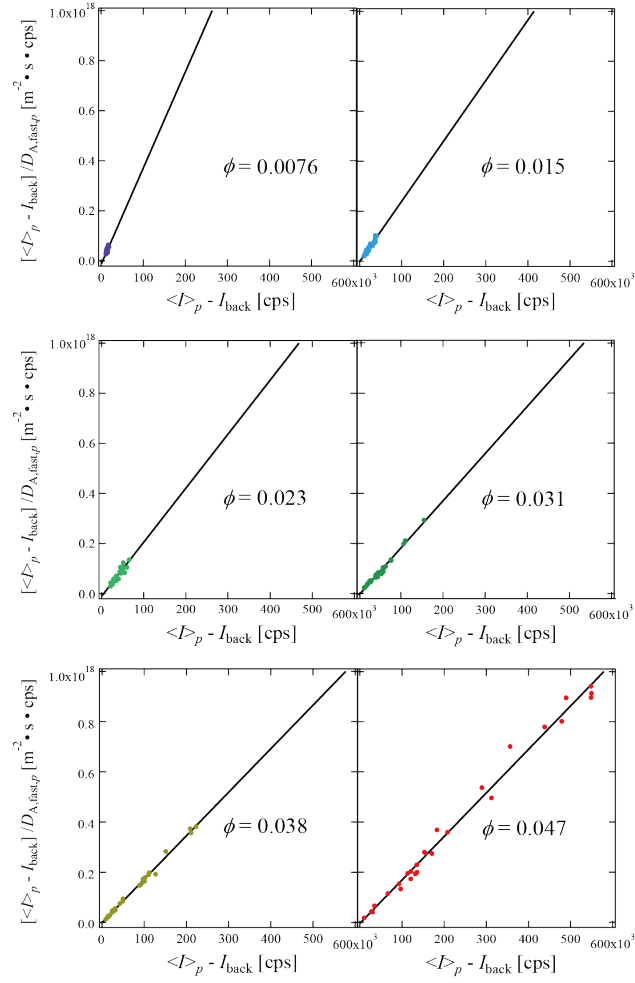
$$D_{fast} = (2 - X_p) D_{A,fast,p} \quad (S8)$$

Based on eq. (S7) and eq. (S8), one can derive the following equation.

$$\frac{\langle I \rangle_p - I_{back}}{D_{A,fast,p}} = \frac{2}{D_{fast}} (\langle I \rangle_p - I_{back}) - \frac{\langle I_F \rangle - I_{back}}{D_{fast}}. \quad (S9)$$

Eq. (S9) indicates that D_{fast} can be obtained from the slope of the plot of $(\langle I \rangle_p - I_{back})/D_{A,fast,p}$ vs $(\langle I \rangle_p - I_{back})$.

Figure S4.



$(\langle I \rangle_p - I_{\text{back}})/D_{\text{A,fast},p}$ vs $(\langle I \rangle_p - I_{\text{back}})$ plots for cellulose in $[\text{C}_2\text{mIm}][\text{CH}_3\text{HPO}_3]$ solutions of various volume fractions.

Figure S4 shows the plots of $(\langle I \rangle_p - I_{\text{back}})/D_{\text{A,fast},p}$ vs $(\langle I \rangle_p - I_{\text{back}})$ for cellulose in $[\text{C}_2\text{mIm}][\text{CH}_3\text{HPO}_3]$ solutions of various volume fractions. Eventually, the correlation length, ξ was estimated from D_{fast} using Einstein-Stokes equation shown in eq. (9) in the main text.

1. Shibayama, M., Universality and Specificity of Polymer Gels Viewed by Scattering Methods. *Bull. Chem. Soc. Jpn.* **2006**, 79, 1799-1819.